Processing flaws and uneven Sentinel-1 coverage distort global flood trend interpretations

Jie Zhao[1,2] (jie.zhao@tum.de), Bernhard Bauer-Marschallinger[1](bernhard.bauer-marschallinger@geo.tuwien.ac.at), Florian Roth[1] (florian.roth@geo.tuwien.ac.at), Davide Festa[1](davide.festa@geo.tuwien.ac.at),

Muhammed Hassaan[1](muhammed.hassaan@geo.tuwien.ac.at), Peter Salamon[3](peter.salamon@ec.europa.eu), Andrea Betterle[3](andrea.betterle@ec.europa.eu), Arjen Haag[4](arjen.haag@deltares.nl),

Patrick Matgen[5](patrick.matgen@list.lu), Marco Chini[5](marco.chini@list.lu), Sandro Martinis[6](sandro.martinis@dlr.de), Xiao Xiang Zhu[2](xiaoxiang.zhu@tum.de), Wolfgang Wagner[1,7] (wolfgang.wagner@geo.tuwien.ac.at)

1 Technische Universität Wien, Vienna, Austria

2 Technical University of Munich, Munich, Germany

3 European Commission, Joint Research Centre, Ispra, Italy

4 Deltares, Delft, the Netherlands

5 Luxembourg Institute of Science and Technology, Luxembourg

5 Deutsche Zentrum f¨ur Luft- und Raumfahrt (DLR), Oberpfaffenhofen, Germany

7 EODC Earth Observation Data Centre, Vienna, Austria

The article was submitted to Nature Communications as a Matters Arising.

Processing flaws and uneven Sentinel-1 coverage distort global flood trend interpretations

Jie Zhao[1,2], Bernhard Bauer-Marschallinger[1], Florian Roth[1], Davide Festa[1], Muhammed Hassaan[1] Peter Salamon[3], Andrea Betterle[3], Arjen Haag[4], Patrick Matgen[5], Marco Chini[5], Sandro Martinis[6] Xiao Xiang Zhu[2], Wolfgang Wagner[1,7]

[1] Technische Universität Wien, Vienna, Austria
[2] Technical University of Munich, Munich, Germany
[3] European Commission, Joint Research Centre, Ispra, Italy
[4] Deltares, Delft, the Netherlands
[5] Luxembourg Institute of Science and Technology, Luxembourg
[5] Deutsche Zentrum für Luft- und Raumfahrt (DLR), Oberpfaffenhofen, Germany
[7] EODC Earth Observation Data Centre, Vienna, Austria

October 27, 2025

Sentinel-1 data has become a desirable data source for global flood mapping due to its wide spatial coverage and weather-independent acquisition. A recent study by [Misra et al., 2025] (hereafter M2025) reported global-scale flood trends based on ten years of Sentinel-1 observations. While the study represents an ambitious attempt to leverage deep learning and synthetic aperture radar (SAR) data for global flood mapping, we raise critical concerns regarding several aspects of its methodology and presentation. In particular, the study's validation protocol, the construction of the exclusion mask, the simplicity of the model architecture, and the missing treatment of the Sentinel-1 coverage heterogeneity, all pose serious questions about the reliability of the reported flood extent products and the resulting global flood trends. Several statements and conclusions drawn from the validation, the method of application in use cases, and trends analyses lack a solid statistical basis and remain unwarranted. In addition, while M2025 briefly references global SAR-based flood mapping efforts, it does not provide a detailed discussion or citation of the Global Flood Monitoring (GFM) archive and exclusion mask/layer. The GFM system, operational since 2021, has delivered near-real-time global Sentinel-1 flood maps and a reprocessed historical archive covering earlier years. Situating AI4G in relation to GFM and similar initiatives would have provided valuable scientific context, clarifying how AI4G extends or differs from existing approaches and helping the broader community assess its contribution to global flood mapping. In this contribution, we contrast the presented results with current scientific challenges in the global detection of flood processes, given their high spatiotemporal dynamics, emphasizing that the underlying issues reflect a fundamental limitation in deriving global flood trends from the temporally and spatially constrained observation of Sentinel-1.

1 Concerns about the dataset validation and case studies

The foundation of M2025 is the AI4G dataset, generated from 10 years of Sentinel-1 intensity data (VV and VH polarizations). A key component of this work is the validation of both the temporally aggregated flood maps and those from individual time stamps. However, the chosen reference datasets raise significant concerns. Table 1 of M2025 compares AI4G aggregated flood map against the Landsat-based GSW dataset [Pekel et al., 2016] and a MODIS-derived flood dataset [Tellman et al., 2021], both of which are suboptimal for flood detection: the GSW product was designed to map permanent water bodies rather than short-duration floods, and inherits observational limitations from the Landsat

archive, including cloud cover, snow, and low solar elevation at high latitudes, which introduce long-term spatial biases [Pekel et al., 2016]; the MODIS-based dataset faces similar constraints from cloud interference and coarse spatial resolution. As M2025 themselves acknowledge, these optical archives carry such limitations; nevertheless, the criterion 'water occurrence less than 50%' used to define flood-prone areas from GSW lacks justification and may not reliably indicate flood susceptibility. Given these limitations, it is expected that a SAR-based product like AI4G would detect more flooded areas, particularly in cloud-covered or rapidly evolving flood situations. Moreover, the authors discuss the partial mismatch and short overlap of the selected products' data periods, but effectively disregard this shortcoming in the presentation of the results (and their statistical meaningful precision). Therefore, the apparent improvement of AI4G over these optical benchmarks does not provide convincing evidence of performance, and the comparison in Table 1 offers limited insight into the actual accuracy or reliability of the AI4G product.

In contrast, the Sentinel-1-based GFM product [Salamon et al., 2021, Wagner et al., 2025] provides the most comprehensive and operationally validated SAR-based global flood maps currently available. We also like to note here that GFM, being embedded in the Copernicus services, provides both an extensive archive of past flood events and flood mapping and near-real-time flood mapping with contextual information in fully automated 24/7-operations. Although M2025 references GFM, it should be noted that M2025 makes appropriate use of both VV and VH polarizations, which can improve flood detection under challenging conditions. In contrast, GFM employs VV polarization only, and comparisons should account for this difference in input configurations. Meanwhile, M2025 does not conduct a proper comparison with its binary flood extent product (as is shown in M2025 Table 3 and Table S2). Instead, it applies a fixed global threshold of 0.3 to the GFM's probabilistic likelihood layer, a value found from an optimisation against the 5 European locations within the KuroSiwo dataset, and uses the resulting maps as input to the global validation. A similar procedure is performed for the AI4G model itself (see M2025 supplementary table S2). While thresholding the GFM likelihood layer can be a valid approach for tailoring flood maps to local conditions [Wagner et al., 2025], applying a single threshold globally is inappropriate because optimal values can vary substantially across regions due to differences in SAR backscatter, land cover, and flood characteristics. Most critically, this approach bypasses the direct use of GFM's operational binary flood maps, which benefit from an ensemble classification grounded in three state-of-the-art algorithms and measures to mitigate over- and under-detection. By tuning the AI4G model on a dataset that is also used for validation, it risks embellishing the results and undermines the credibility of the comparison. Finally, the KuroSiwo dataset focuses primarily on Europe, making it inadequate as a reference for evaluating a global-scale flood mapping model.

To get an idea of AI4G's performance, we conducted an exemplary test on the prominent 2021 Central European flood event. Similar to examples in Belgium and Germany, GFM v3.2 accurately delineates the flood extent in Luxembourg, whereas AI4G significantly underestimates it (Figure 1). The unfiltered AI4G output fragments the flood into spare, jagged patches and applying the recommended filters (particularly in the east section of the flood the moisture anomaly filter) further reduces detected flood surface. From a SAR perspective, this case is particularly concerning, as the event is known to be an 'easy' event for Sentinel-1 flood mapping, with a large-scale extent, a good SAR image contrast against wet soils, a low overall fraction of dense vegetation or challenging topography, and a good temporal overpass match. The AI4G method includes the application of an 80 m buffer to the classification results (impact can be seen in Figure 4) to mitigate physical effects leading to underestimation of SAR-based methods. While the paper acknowledges potential causes of underestimation, none of these factors are evident in this case. Instead, the SAR backscatter data could support the retrieval of a more accurate flood map with finer details, as demonstrated by the GFM results. That said, the shared AI4G dataset does not include this buffer, and the filtered classification result lacks sufficient seed points for effective buffer application across most of the flood surface. This suggests that the AI4G model may not fully capture certain major flood events, even in well-observed regions, indicating potential limitation in the representativeness of the validation.

Then again, AI4G also shows systematic overestimation in other regions. In M2025's example shown for Ethiopia, large portions of the mapped floods coincide with permanent or seasonal water bodies when compared with GSW and GFM reference water masks (Figure 2). Fig. 2 is based on the AI4G data as described in the readme file added by the authors on 2025-Oct-13, clarifying the value-encoding of the distributed data. The example from Kenya shows widespread detections overlap

regions where no floods were reported at all (Figure 3, most notable in the eastern half of Kenya), neither by the radar-based GFM, nor by the optical-based Suomi-NPP/VIIRS [Li et al., 2018] service.

These examples, combined with the static exclusion mask, show that AI4G may overestimate floods in some areas while underestimate them in others. When considered together, this patterns suggest potential biases in the reported validation. Consequently, the 'additional' flooded area in M2025 Table 1 may be overstated, and the claimed precision should be interpreted with caution given the current validation setup.

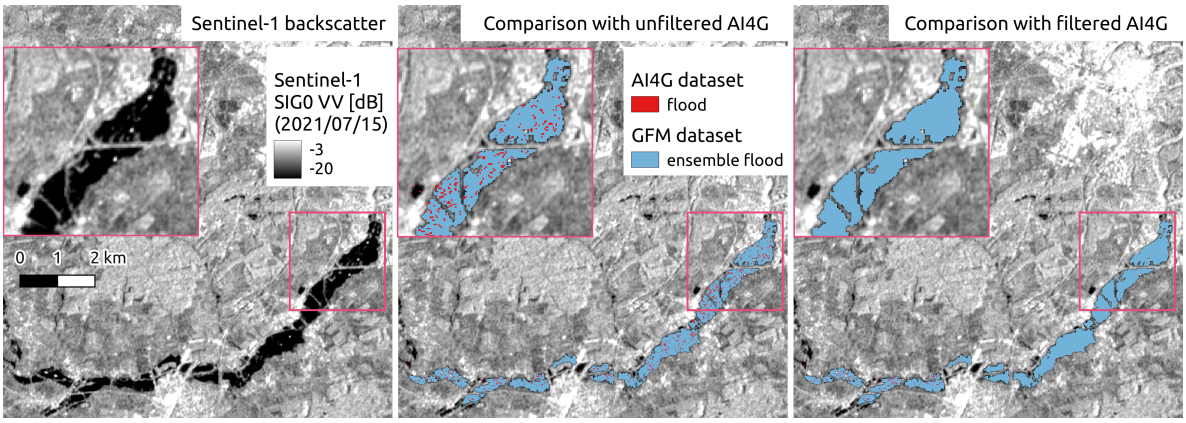

Figure 1: Comparison for a section of the 2021 Central European flood event in Luxembourg, an example of serious underestimation of AI4G dataset.

2 Uncertainties introduced by post-processing procedures

M2025 describes two types of post-processing: one to filter out potential false positives using time-varying auxiliary data and static features, and another in the form of a static exclusion mask intended to identify areas where flood detection may be unreliable due to either false positives or false negatives. In M2025, AMSR-2 soil moisture and ERA5 land surface temperature are used to exclude areas with low moisture or freezing conditions. However, both datasets have coarse spatial resolution and known limitations that reduce their suitability for heterogeneous landscapes. In particular, passive-microwave soil-moisture retrievals, such as AMSR-2, are known to be unreliable over standing water and inundated soils, often producing biased estimates due to surface water interference. Using such data as an exclusion criterion thus risks unintentionally masking true floods. Moreover, the use of global thresholds lacks statistical justification and does not reflect environmental differences across regions. Furthermore, the switching between retrieval algorithms based on expert judgment, combined with limited diversity in the training data, may affect the robustness and generalizability of the post-processing approach. Notably, AMSR-2 was chosen over more accurate alternatives such as SMAP or the ESA CCI multi-sensor soil moisture product, both of which generally outperform AMSR-2 in global validation studies and also offer comparatively higher spatial resolution. This choice may further constrain the exclusion mask's ability to represent actual soil moisture conditions across diverse environments.

Another concern is raised for the static exclusion mask. The distinction between 'static features' and the 'static exclusion mask' is ambiguous and partially redundant. The exclusion mask reportedly includes bare ground, built-up areas, and steep slopes (>10°) based on GLO-30 and ESA WorldCover data. However, the main text refers to 'bare ground', while the supplementary materials specify 'Bare/Sparse Vegetation', which are not equivalent classes in ESA WorldCover. Additionally, the model validation section notes that dense forests should be excluded due to SAR limitations, yet this is not reflected in the exclusion mask description or post-processing steps. ESA WorldCover underpins the post-processing mask, while the Ethiopia case study employs the ESRI land-cover map without explanation. Meanwhile, in SAR data, flood detection over bare ground or sparse vegetation is generally feasible and should not be excluded by exclusion mask. All those inconsistencies in land cover class definitions and implementation create confusion regarding the actual construction and reproducibility

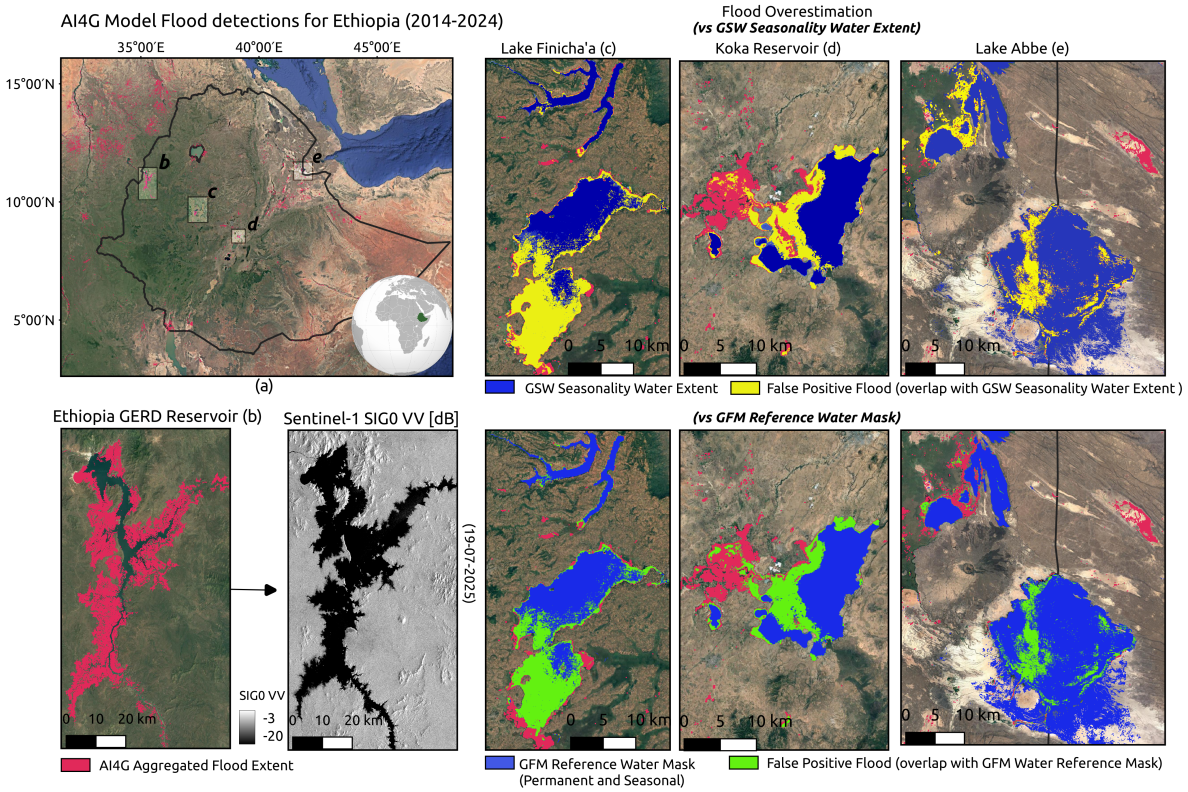

Figure 2: AI4G model flood extent detections and overestimation analysis for Ethiopia (2014–2024). (a) Aggregated flood extent detected by the AI4G model across Ethiopia over the period. (b) Detailed view of the GERD reservoir area with AI4G flood extent shown in red, with Sentinel-1 SIG0 VV backscatter imagery of the GERD reservoir region acquired on 19 July 2025. (c) Zoomed-in view on Lake Finicha'a area. AI4G floods overlap largely with the GSW dataset (upper panel) and the GFM reference water mask (lower panel), indicating that much of the detected flooding corresponds to permanent or seasonal water bodies. (d) same as (c) for Koka Reservoir area. (e) same as (c) for the eastern region along the border with Djibouti, covering the Lake Abbe area.

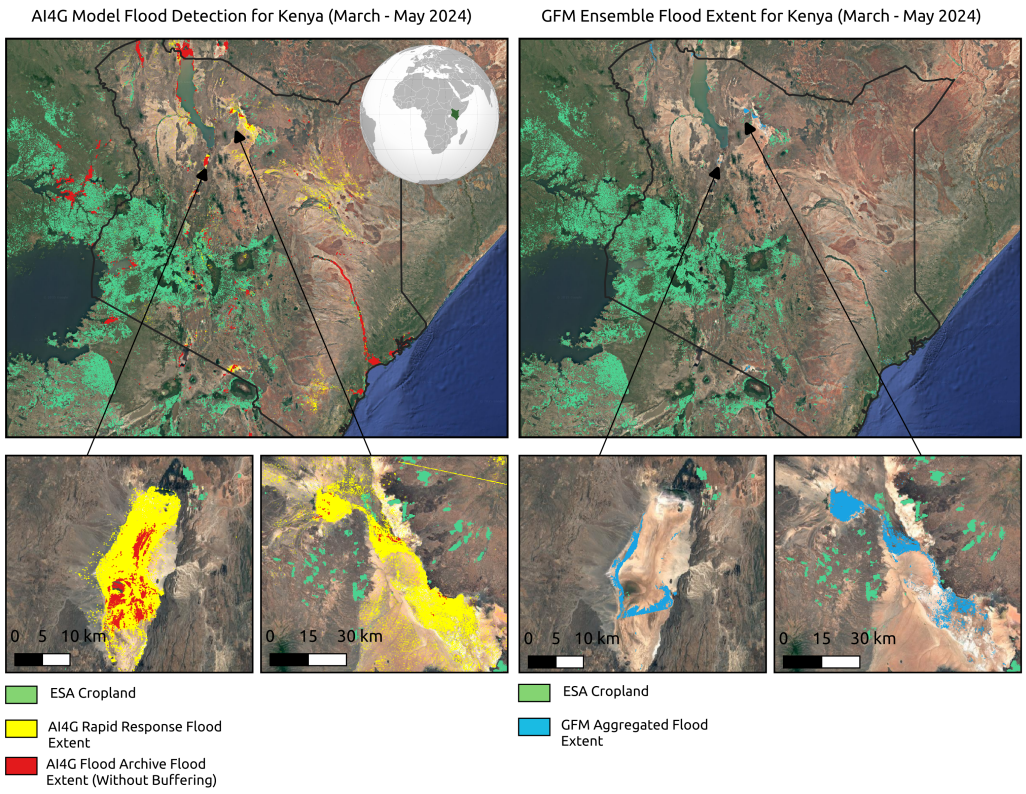

Figure 3: An example of overestimation in Kenya: Rapid-response results from M2025 overlaid with aggregated AI4G flood archive data, which shows a much lower flood extent. On the right for comparison, the GFM aggregated data based on the GFM archive (March - May 2024).

of the exclusion logic.

Particularly, the overestimation observed in Ethiopia and Kenya directly reflects these post-processing issues. Three representative examples from Ethiopia are shown in Figure 2, where AI4G detected floods coincide substantially with permanent or seasonal water bodies, as confirmed by GSW seasonality water extent (based on observations from 2021) and GFM reference water masks (based on 2017-2021). The ESA product used to mask permanent water defines it as areas covered for more than nine months per year but omits seasonal dynamics, leading to frequent misclassification of seasonal lakes and wetlands as floods. This problem is compounded by AI4G's change-detection step, which allows up to 30 days between pre- and post-event acquisitions. Such long intervals can easily span seasonal transitions (e.g., from dry to rainy season), so the model may label water bodies as 'flooded' even if they are part of normal seasonal variation. In some cases, this occurs even when the pre- and post-event backscatter is similar, indicating that the algorithm is not effectively distinguishing permanent or seasonal water from true floodwater. A similar problem appears in Figure 2 (b), showing a zoom-in of the Grand Ethiopian Renaissance Dam (GERD) reservoir, which has been a permanent water body since 2020 but is still mapped by AI4G as flooded. It is worth noting that similar inconsistencies appear not only over GERD reservoir but also across other lakes with seasonal dynamic boundaries, where natural water surface variations are misinterpreted as flooding (e.g. as in Fig. 2 c and e). As for example also GFM partially misattributes the filling of GERD as flood, these examples highlight a broader challenge in global flood mapping, that accurately distinguishing dynamic surface water changes from floodwater remains a key unresolved problem, and underline the need for more accurate and up-to-date reference water masks to reduce systematic overestimation. Notably, using as described in M2025 the GSW water occurrence—which is based on the 1984-2021 period—to define flood-prone areas and contrast them against individual recent flood events introduces a methodological inconsistency, as newer permanent water bodies may consequently be misclassified as floods.

Another overestimation pattern is observed in Kenya, where AI4G substantially detected more floods when compared to GFM products (Figure 3). Further, the figure reveals inconsistencies between the rapid response results shown in Figure 5 of M2025 and their AI4G flood archive data, which indicates a much smaller extent of flooding. These examples further illustrate how current post-processing limitations affect the consistency and reliability of AI4G flood records across regions.

Moreover, the conceptual framing and implementation of the exclusion mask in M2025 diverge from earlier work that established its theoretical foundation. Previous research has developed two versions of SAR-based exclusion masks: a globally applicable expert-curated version used operationally in the GFM product [Wagner et al., 2025], and a fully automated version based on Sentinel-1 orbit geometry [Zhao et al., 2021]. A subsequent study systematically compared these two approaches, analyzing their suitability for global-scale applications [Zhao et al., 2023]. These efforts defined the exclusion mask not merely as a tool for suppressing false positives, but as a principled method for delineating regions where SAR backscatter is inherently unreliable for flood detection, such as in topographic shadow/layover, dense vegetated areas, or persistently dry zones. Its broader relevance has also been discussed in the context of soil moisture retrieval (i.e., Chapter 5 of van Hateren's doctoral dissertation [van Hateren, 2023]). In contrast, M2025 applied the exclusion mask primarily as a filtering step for false alarm removal, without referencing these prior conceptual frameworks, which limits the scientific transparency of their method and does not fully reflect the original purpose and potential of the exclusion mask approach.

While M2025 does not explicitly discuss this step as post-processing, a buffer or dilation of 80 m or 240 m is applied subsequent to the initial flood classification. As illustrated in Figure 1, the initial classification tends to underestimate the flood extent in a jagged and patchy manner, what appears to be the motivation behind applying the circular buffer. However, this empirical adjustment does not directly address the underlying classification errors. Not only does it overlook the original SAR signal, but it also effectively enlarges the minimum mapping unit for flood mapping without a clear physical or statistical justification. Figure 4 shows how the applied buffer accounts for a large part of the found flood of the Ethiopia example of M2025.

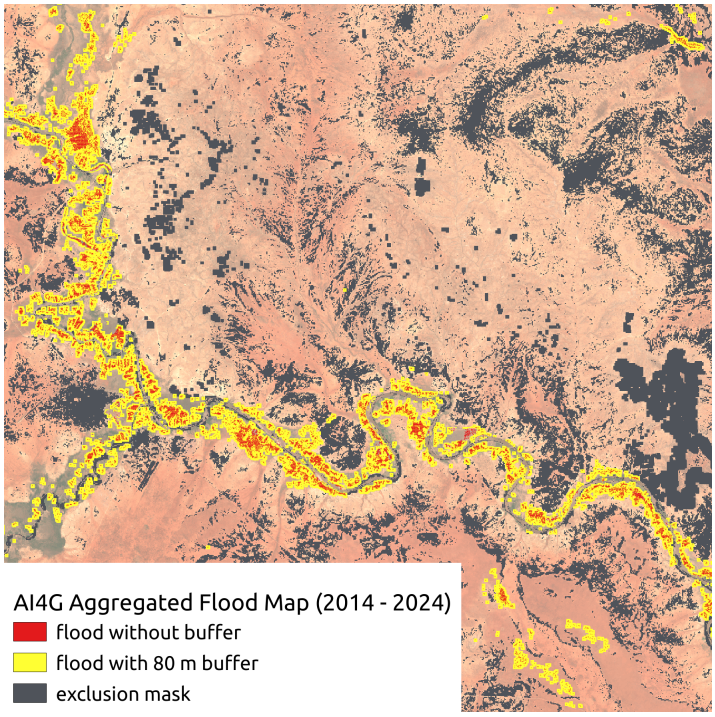

Figure 4: Visualization of 80 m buffer for aggregated flood map (2014-2024) of the Ethiopia example.

3 Concerns about the over-simplified CNN model for a globally complex flood mapping task

M2025 uses a U-Net architecture with a MobileNetV2 encoder for flood detection. The model is trained and validated on only four flood events: Pakistan (August 2022) and Greece (September 2023) for training, Mozambique (March 2023) for validation, and Southeast Ethiopia (November 2023) for testing. For a global flood mapping task, this limited number of training events provides only a narrow basis for generalization. The training set lacks geographic and environmental diversity, which constrains the model's ability to generalize to different regions and conditions. In particular, none of the training samples shares the geomorphological or climatic characteristics of central Europe, a gap that likely contributes to the model's failure to capture the 2021 Luxembourg flood (Figure 1) and potentially many similar events. Meanwhile, the number of sample for model training has not been reported yet. Based on our experience, two flood events are insufficient to support a model intended for global applications, even with data augmentation. Such augmentation can introduce distributional artifacts and lead to overfitting in regions not represented in the training data.

The AI4G model proposed in M2025 relies on handcrafted features such as binary change indicators and delta backscatter amplitudes, rather than directly using raw pre- and post-event SAR intensities. The authors justify this design by citing improved performance under limited training data. However, with the release of the global-scale S1GFloods dataset in 2023 [Saleh et al., 2024], which includes paired Sentinel-1 images and pixel-level flood labels for 46 events worldwide, this constraint no longer applies. S1GFloods provides exactly the input structure needed for a fully learnable, end-to-end flood detection model that can directly extract relevant patterns from raw intensities. Continuing to rely on handcrafted heuristics under these conditions limits the model's adaptability and scalability. In addition, AI4G is a change detection approach that does not appear to account for long-duration events in which floodwater is already present in the reference image. M2025 would benefit from clarifying how reference selection and differencing handle pre-existing inundation and quantify any resulting bias if this case is left unaddressed.

4 Structural constraints in deriving global flood trends from limited and uneven observations

M2025 claims to provide a globally consistent, observation-driven view of flood dynamics over time. However, the trend analyses presented in M2025's Table 2 and Figure 7 rest on several conceptual and methodological issues that challenge the validity of the reported trends.

The spatial and temporal coverage of Sentinel-1 is highly heterogeneous, due to fixed orbit configurations, regionally variable acquisition strategies, and changes in satellite constellation, including the early single-satellite phase and the loss of Sentinel-1B in 2021. These inconsistencies (Figure 5) are only superficially addressed through a simple normalization based on acquisition count. The authors do acknowledge inter-annual variation, but assess its impact only through global p-values derived from three selected scenarios presented around M2025 Table 2, which is insufficient to account for the full extent of temporal and spatial coverage biases. Also, the reported cell-based trends in M2025 Figure 7 lack confidence intervals and fail to consider uneven sampling, which, together with the short 10-year record, limits their statistical robustness. Most critically, the extrapolation of a 5% annual increase to a 60% rise per decade is not statistically substantiated, particularly given the limited data duration and unquantified uncertainties. A meaningful long-term trend analysis would require a longer, more homogeneous, and consistently acquired high-resolution satellite observation archive. This prerequisite is currently not met in the context of SAR-based flood mapping. Tarpanelli et al. [2022] carried out a dedicated study and analysed flood processes with discharge time series, and they found that even over Europe only 58% of flood events (on average) are potentially observable by Sentinel-1 at the current two satellite constellation. Given these limitations, neither the data nor the methodology supports conclusions about the direction or magnitude of global flood change.

Another major issue lies in the treatment of floods as a homogeneous phenomenon. Floods vary greatly in extent, duration and recurrence, and a reliable trend analysis requires a balanced registration of these properties. However, the AI4G product's coarse structure (the monthly aggregation and spatial buffering) limits its ability to capture flood dynamics across diverse temporal and spatial scales. As short-living peak floods, persistent inundations, and seasonal water bodies are all treated the same within the monthly aggregated extent layers, the dataset in its current form cannot resolve flood dynamics and frequency sufficiently. Above all, this blending of different hydrological phenomena complicates the interpretation of the results. Here, single extreme events can dominate the signal in a region and create the illusion of long-term change. For instance, major floods in China such as those in Zhengzhou (2021) and Beijing/Hebei (2023) leave visible signals in M2025 Figure 7. In contrast, persistent increases in flood activity observed in southeast China [Lu et al., 2025] are not reflected, indicating that the trend map may overemphasize isolated extremes while failing to reflect gradual or recurrent flood intensification. In summary, the data behind M2025 Table 2 and Figure 7 mixes fundamentally different types of hydrological events and thus limits their suitability for robust flood trend analyses.

Finally, the use of dynamic exclusion masks based on soil moisture and temperature introduces the risk that variations in environmental thresholds, rather than actual hydrological change, drive the observed trends. A thorough uncertainty and sensitivity analysis that separates true hydrological signals from the substantial and heterogeneous observation gaps, masking effects, and sampling biases is absent. Without such analysis, a global trend map such as that in M2025 Figure 7 cannot be interpreted as evidence of genuine regional flood change.

5 Other issues

M2025 tends to use the AI4G product for flood risk application where Ethiopia and Kenya have been used as application test cases. In the case of Ethiopia, it is reasonable that flood risks exists in rainfed agricultural zones. However, the approach in M2025 to assess such risk is highly simplistic, relying on the spatial overlay of historical SAR-based flood detections with a generic cropland layer. This method lacks temporal context, such as cropping calendars or growth stages and does not include ground-truth validation or independent evidence. As a result, the analysis provides limited actionable insight, and the claim of identifying flood-prone agricultural areas remains insufficient to support risk-informed decision-making.

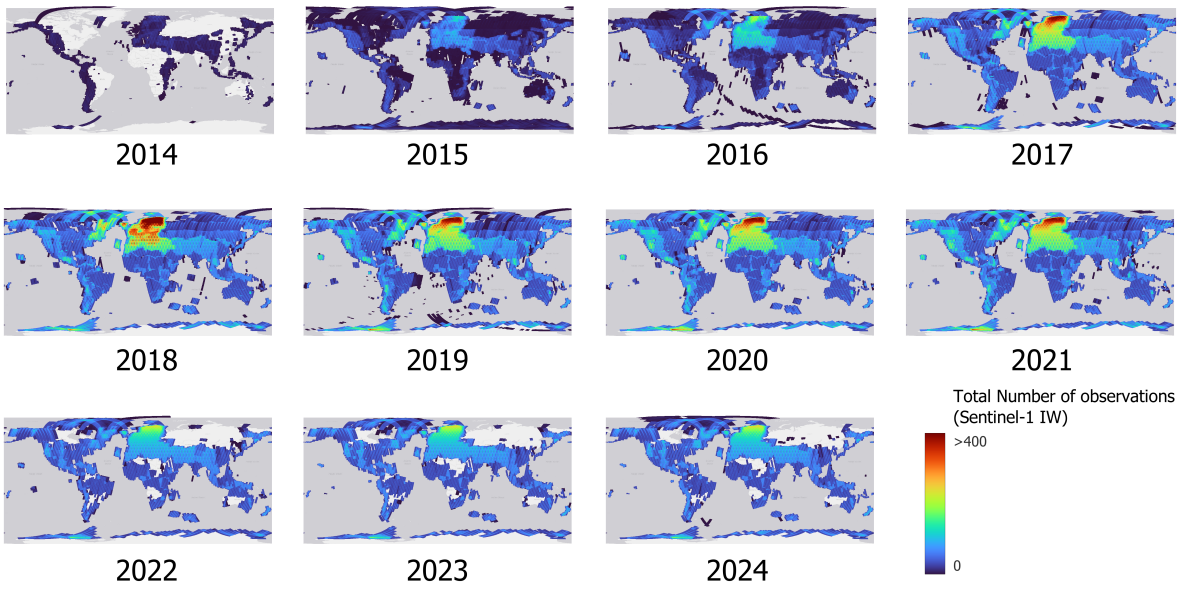

Figure 5: Total number of Sentinel-1 IW acquisitions per year (2014–2024).

Moreover, the authors refer to 'amplitude' data from Sentinel-1 throughout the paper, while the input data used for both model training and inference appear to be intensity images (i.e., power-scaled backscatter, typically in dB). While amplitude and intensity are related, they are not interchangeable: intensity is the square of amplitude, and their statistical behavior (particularly in speckle characteristics and image processing) is different. Clarifying this distinction is important for methodological transparency and for avoiding potential confusion among readers less familiar with SAR data.

Authors Contributions

Conceptualization: J.Z., B.B.M., F.R., D.F., M.H., P.S., A.B., A.H., W.W. Writing – Original Draft: J.Z., B.B.M., F.R., D.F., M.H. Writing – Review & Editing: J.Z., B.B.M., F.R., D.F., M.H., P.M., M.C.,S.M., X.X.Z. W.W. Visualization: J.Z., F.R., D.F., M.H.

References

Sanmei Li, Donglian Sun, Mitchell D Goldberg, Bill Sjoberg, David Santek, Jay P Hoffman, Mike DeWeese, Pedro Restrepo, Scott Lindsey, and Eric Holloway. Automatic near real-time flood detection using suomi-npp/viirs data. *Remote sensing of environment*, 204:672–689, 2018.

Zhenghui Lu, Linhao Zhong, Yang Yang, Xinlei Han, Xiaoling Jiang, Zitong Shi, and Dabang Jiang. Spatial characteristics and connectivity of urban floods in eastern china: Insights from a newly established data set during 2010–2020. *Geophysical Research Letters*, 52(1):e2024GL113017, 2025.

Amit Misra, Kevin White, Simone Fobi Nsutezo, William Straka III, and Juan Lavista. Mapping global floods with 10 years of satellite radar data. *Nature Communications*, 16(1):5762, 2025.

Jean-François Pekel, Andrew Cottam, Noel Gorelick, and Alan S Belward. High-resolution mapping of global surface water and its long-term changes. *Nature*, 540(7633):418–422, 2016.

Peter Salamon, Niall Mctlormick, Christopher Reimer, Tom Clarke, Bernhard Bauer-Marschallinger, Wolfgang Wagner, Sandro Martinis, Candace Chow, Christian Bohnke, Patrick Matgen, Marco Chini, Renaud Hostache, Luca Molini, Elisabetta Fiori, and Andreas Walli. The New, Systematic Global Flood Monitoring Product of the Copernicus Emergency Management Service. In *2021 IEEE International Geoscience and Remote Sensing Symposium IGARSS*, pages 1053–1056, Brussels, Belgium, July 2021. IEEE. ISBN 978-1-6654-0369-6. doi: 10.1109/IGARSS47720.2021.9554214. URL https://ieeexplore.ieee.org/document/9554214/.

Tamer Saleh, Xingxing Weng, Shimaa Holail, Chen Hao, and Gui-Song Xia. Dam-net: Flood detection from sar imagery using differential attention metric-based vision transformers. *ISPRS Journal of Photogrammetry and Remote Sensing*, 212:440–453, 2024.

Angelica Tarpanelli, Alessandro C Mondini, and Stefania Camici. Effectiveness of sentinel-1 and sentinel-2 for flood detection assessment in europe. *Natural Hazards and Earth System Sciences*, 22 (8):2473–2489, 2022.

Beth Tellman, Jonathan A Sullivan, Catherine Kuhn, Albert J Kettner, Colin S Doyle, G Robert Brakenridge, Tyler A Erickson, and Daniel A Slayback. Satellite imaging reveals increased proportion of population exposed to floods. *Nature*, 596(7870):80–86, 2021.

T.C. van Hateren. *Soil moisture droughts evaluated using Earth observation*. PhD thesis, Wageningen University, 2023. URL https://library.wur.nl/WebQuery/wurpubs/621431.

Wolfgang Wagner, Bernhard Bauer-Marschallinger, Florian Roth, Tobias Stachl, Christoph Reimer, Niall McCormick, Patrick Matgen, Marco Chini, Yu Li, Sandro Martinis, Marc Wieland, Franziska Kraft, Davide Festa, Muhammed Hassaan, Mark Edwin Tupas, Jie Zhao, Michaela Seewald, Michael Riffler, Luca Molini, Richard Kidd, Christian Briese, and Peter Salamon. The fully-automatic sentinel-1 global flood monitoring service: Scientific challenges and future directions. *SSRN Preprint*, 2025. doi: 10.2139/ssrn.5110703. URL https://ssrn.com/abstract=5110703. Submitted to *Remote Sensing of Environment*, major revisions requested.

Jie Zhao, Ramona Pelich, Renaud Hostache, Patrick Matgen, Senmao Cao, Wolfgang Wagner, and Marco Chini. Deriving exclusion maps from c-band sar time-series in support of floodwater mapping. *Remote Sensing of Environment*, 265:112668, 2021.

Jie Zhao, Florian Roth, Bernhard Bauer-Marschallinger, Wolfgang Wagner, Marco Chini, and Xiao Xiang Zhu. A preliminary comparison of two exclusion maps for large-scale flood mapping using sentinel-1 data. *ISPRS Annals of the Photogrammetry, Remote Sensing and Spatial Information Sciences*, 10:911–918, 2023.